A Novel 36,000-dalton Actin-binding Protein Purified from Microfilaments in *Physarum* Plasmodia Which Aggregates Actin Filaments and Blocks Actin-Myosin Interaction

SATOSHI OGIHARA and YUJI TONOMURA
Department of Biology, Faculty of Science, Osaka University, Osaka 560, Japan

ABSTRACT In the plasmodia of *Physarum polycephalum*, which show a cyclic contraction-relaxation rhythm of the gel layer, huge aggregates of entangled actin microfilaments are formed at about the onset of the relaxation (R. Nagai, Y. Yoshimoto, and N. Kamiya. 1978. *J. Cell Sci.* 33:205–225). By treating the plasmodia with Triton X-100, we prepared a demembranated cytoskeleton consisting of entangled actin filaments and found that the actin filaments hardly interact with rabbit skeletal myosin. From the cytoskeleton we purified a novel actin-binding protein which binds stoichiometrically to actin and makes actin filaments curled and aggregated. It also inhibits the ATPase activity as well as the superprecipitation of reconstituted rabbit skeletal muscle actomyosin. This protein has a polypeptide molecular weight of 36,000 and binds 7 mol of actin/mol 36,000 polypeptide.

Actin filaments are a major component of the cytoskeletal apparatus in nonmuscle cells (1, 2), and their supramolecular organization differs conspicuously from one form of cytoskeleton to another (e.g., bundles as seen in stress fibers [3], retraction fibers [4], microvilli of intestinal epithelial cells [5], sea urchin eggs [6], sea urchin coelomocytes [7], the contractile ring [8], and *Nitella* cells [9], or meshworks as seen in the ingestion act of macrophages [10] and the ruffling region of culture cells [11]). Recent studies from several approaches have revealed roles of actin-binding proteins in the formation of such specific organization of the microfilaments (12–19). On the other hand, differences in microfilament morphology also occur, being coupled with contraction and/or relaxation phenomena in some cell systems (20–23), among them the plasmodia of *Physarum polycephalum* upon which much attention has been focused because of the distinctness of its coupling.

In 1964, Wohlfarth-Bottermann (24) reported a clear correlation between the microfilament population and the direction of the cytoplasmic streaming. The birefringent fibrils (25) were found by Kamiya (26) to appear and disappear cyclically in accordance with the shuttle streaming. Recently, we demonstrated the inclusion of actin filaments in the birefringent fibrils (27). The above reports all make it highly probable that the actin-containing fibrils are well oriented, showing strong birefringence in the contraction phase and becoming nonbirefringent in the relaxation phase.

As to why the microfilaments are nonbirefringent in the relaxation phase, Nagai et al. (20) claimed that at about the onset of the relaxation most of the microfilaments are entangled, forming networks. We thought that some actin-binding protein might be responsible for the specific entangled microfilaments and that it would cut off the interaction between actin and myosin. To try to understand the microfilament morphology change which might be coupled with the contraction-relaxation phenomena in terms of alterations in the interactions among actin, myosin, and other protein components, we developed a new procedure for isolating the entangled microfilaments from the plasmodia. The obtained fraction resembled the microfilaments observed in the relaxation phase in vivo (20) and contained actin as a major component but did not interact with myosin, indicating that the actin filaments in this fraction were made relaxation-quiescent by the procedure employed. From this fraction we purified a novel actin-binding protein, a 36,000-dalton polypeptide. This protein made actin filaments curled and cross-linked to form large masses and inhibited the actin-myosin interaction. We also found evidence that this protein is not tropomyosin.

MATERIALS AND METHODS

Preparation of Crude F-Actin Fraction

The plasmodia of *P. polycephalum* were cultured by the method of Camp (28), with slight modifications. To 100 g of the plasmodia was added 1,000 ml of an

THE JOURNAL OF CELL BIOLOGY · VOLUME 93 JUNE 1982 604-614

ice-cold Triton solution consisting of 0.5% Triton X-100, 10 mM EGTA, 10 mM dithiothreitol (DTT), 0.1 mM phenylmethylsulfonyl fluoride (PMSF), 10 mM NaF, 10 mM Na-pyrophosphate, and 25 mM K-phosphate buffer at pH 7.0. The mixture was then stirred gently for 15 min on ice with a magnetic stirrer, the pH being adjusted carefully to 7.0 with 1 M KOH. The mixture was centrifuged at 1,000 *g* for 10 min at 4°C, and the precipitate was again mixed with the same volume of Triton solution as before and subjected to stirring and then centrifugation as described above. The second precipitate was washed twice with 1,000 ml of an ice-cold washing solution, the constituents of which were the same as the Triton solution except that 10 mM EDTA and 10.1 mM $CaCl_2$ were substituted for Triton X-100 and EGTA. We call the final precipitate the crude F-actin fraction. We paid careful attention to possible proteolysis during the preparation, e.g., by separating the initial precipitate rapidly from the soluble fractions and by adding 0.01–0.1 mM PMSF to all the solutions used. Prolonged mixing without PMSF caused breakdown of the polypeptides, especially higher molecular ones, judging by SDS PAGE.

Isolation of 36,000-dalton Factor from the Crude F-Actin Fraction

To the crude F-actin fraction suspended in the washing solution, 0.25 volume of 3 M KI was added and the pH was slowly raised to 8.2 with 1 M KOH. The mixture was homogenized with a motor-driven tight-fitting Pierce homogenizer (Pierce Chemical Co., Rockford, IL) with a Teflon pestle with ten passes. The homogenate was stirred on ice for 60 min and centrifuged at 125,000 *g* for 90 min at 4°C. The supernatant solution was dialyzed against 50 mM KCl, 1 mM DDT, 10 μM PMSF, and 10 mM imidazole-HCl buffer at pH 6.5 with several changes of the solution. Fluffy material which formed during the dialysis was removed by centrifugation at 6,000 *g* for 10 min. To the supernatant solution (fraction I), 50% saturated ammonium acetate at pH 8.0 and 0°C was added dropwise, and then the mixture was stirred for 25 min on ice and centrifuged at 78,000 *g* for 30 min at 4°C. The supernate thus obtained in 21.4% saturation was dialyzed against 50 mM KCl, 1 mM DTT, 10 μM PMSF, and 10 mM imidazole-HCl at pH 7.0 to remove ammonium acetate, then condensed (fraction II) with an Immersible CX Kit (Millipore Corp., Bedford, MA) and Lyphogel (Gelman Sciences, Inc., Ann Arbor, MI) and subjected to gel filtration on a 1.3 x 30 cm column of Sephacryl S-300 Superfine equilibrated and eluted with 0.6 M KCl, 1 mM DTT, 10 μM PMSF, and 10 mM imidazole-HCl at pH 7.0 and 2°C at the flow rate of 54 ml/h. The elute was collected in 1 ml/fraction and all the fractions were assayed for the inhibitory activity in the superprecipitation of reconstituted skeletal actomyosin. Appropriate fractions with the inhibitory activity (*cf.* Fig. 5) were pooled and passed through an activated charcoal column (0.7 x 1.5 cm) to remove contaminant RNA. The elute was condensed with an Immersible CX-Kit and Lyphogel, and an aliquot was rechromatographed on a smaller column of Sephacryl S-300 (0.84 x 18 cm) with the same elution buffer. Fractions of 0.25 ml/tube were collected and the 36,000-dalton polypeptide was eluted from the column as a single symmetric peak with slight contamination by RNA. Fractions across the peak obtained were pooled and used in the experiments.

Myosin, Actin, Tropomyosin, and Troponin

Myosin, heavy meromyosin (HMM), and actin were prepared from rabbit skeletal muscle by the methods of Perry (29), Szent-Györgyi (30) and Spudich and Watt (31), respectively. Tropomyosin was isolated from the native tropomyosin fraction of rabbit skeletal muscle (32) by forming paracrystals in 50 mM $MgCl_2$ and collecting them as a low-speed pellet. Tropomyosin and troponin for direct binding study were prepared from rabbit skeletal muscle following the methods of Ebashi et al. (33). Tropomyosin was further purified by repeating three times the isoelectric precipitation at pH 4.7 in 0.4 M LiCl and ammonium sulfate fractionation. Pure troponin was obtained by precipitation in 2 M urea at pH 5.35 (34). Gizzard tropomyosin was kindly supplied by Mitsuo Ikebe of our laboratory. Plasmodial actin was prepared following the method of Hatano and Owaribe (35).

Activation of the Mg-ATPase Activity of Myosin by the Crude F-Actin Fraction

Skeletal myosin in 0.5 M KCl was mixed with pure plasmodial F-actin or the crude F-actin and then diluted with an appropriate solution to give the final concentrations of 50 μg/ml myosin, 0–0.075 mg/ml pure F-actin, 0–0.44 mg/ml crude F-actin, 0.1 mM $MgCl_2$, 50 mM KCl, and 20 mM imidazole-HCl buffer at pH 7.0 at 20°C. The reactions were started by the addition of 50 μM ATP and stopped after 0–45 s with 5% trichloroacetic acid (TCA). The rate of the ATPase reaction was determined by measuring the rate of phosphate liberation by the method of Martin and Doty (36).

HMM Binding to the Crude F-Actin Fraction

A sample of 0.16 mg/ml crude F-actin was mixed with various concentrations of skeletal muscle HMM (0.03–0.27 mg/ml) in 50 mM KCl, 5 mM DTT, 50 μM PMSF, and 30 mM imidazole-HCl buffer at pH 7.0 for 15 min at 15°C. The mixture was then ultracentrifuged. The clear supernatant solution which contained unbound HMM was separated from the small dense pellet which contained the complex of HMM and the actin in the crude F-actin fraction. The amount of free HMM was determined by measurements of the K-EDTA ATPase activity of the supernate in 0.5 mM ATP, 0.5 M KCl, 5 mM EDTA, 2.5 mM DTT, 25 μM PMSF, and 15 mM imidazole-HCl buffer at pH 7.0 at 20°C. The amount of bound HMM was determined, for accuracy, by comparing the ATPase activity of the supernates in the presence and in the absence of the crude F-actin fraction. A control experiment was done under similar conditions with a combination of 0.1 mg/ml pure plasmodial F-actin and 0–2.4 mg/ml HMM.

SDS Gel Electrophoresis

Disk electrophoresis of various preparations was performed on 7.5% SDS polyacrylamide gels according to the method of Weber and Osborn (37), with slight modifications (38). When samples were dilute and/or contained high concentrations of K ions, they were lyophilized, suspended in small amounts of distilled water, and dialyzed overnight against 1% SDS, 23.3% glycerol, 0.006% Bromophenol Blue, and 10 mM Na-phosphate buffer at pH 7.0, followed by solubilization by heat in the presence of 7.7% β-mercaptoethanol (β-ME). The gels were stained with Coomasie Brilliant Blue and scanned with a densitometer equipped in a Gilford Spectrophotometer 250 (Gilford Instrument Laboratories, Inc., Oberlin, OH) at the wavelength of 570 nm.

Protein Concentrations

Protein concentrations were determined either by the biuret reaction (39) or by the method of Lowry et al. (40) with bovine serum albumin (BSA) as a standard. When reducing agents were present, proteins were coprecipitated with 0.017% deoxycholic acid (DOC) in 6% TCA (41) and then analyzed by the method of Lowry et al. (40). For troponin binding study, the microbiuret method (42) was used.

Optical Methods and Electron Microscopy

The crude F-actin fraction was observed with a Zeiss Photo II with polarizing equipment as described previously (27). For electron microscopy, the fraction was fixed at room temperature with 2% glutaraldehyde in 50 mM KCl and 10 mM K-phosphate buffer at pH 7.0 for 100 min. It was then washed twice, postfixed in 1% OsO_4, 50 mM KCl, and 10 mM K-phosphate buffer at pH 7.0 at room temperature for 60 min, and embedded in Spurr's resin after dehydration with an alcohol series. Thin sections were stained with 25–30% uranyl acetate followed by lead citrate and observed with a JEM 100-C electron microscope at 80 kV. For negative staining, samples were diluted with the appropriate solutions and applied immediately to a Formvar-coated grid and stained with 1–2% uranyl acetate.

RESULTS

Crude F-Actin Fraction

As a large mass of the plasmodia was stirred in the Triton X-100 solution to prepare the crude F-actin fraction, the yellow pigment peculiar to the *Physarum* plasmodia gradually dissolved away, and the plasmodia became whitish after exhaustive washing. During the treatment, the plasmodia were fragmented into small pieces of several hundreds of microns. The crude F-actin consisted mostly of amorphous aggregates of a material elastic enough to allow immediate recovery of the original shapes even when they were pressed with a cover glass or stretched with tweezers. Note that the amorphous aggregates (Fig. 1 *a*) showed no significant birefringence under polarized light (Fig. 1 *b*). The remaining, very small part of the population were rod-shape aggregates of phase-dense material (Fig. 1 *c*) and showed strong birefringence (Fig. 1 *d*). The presence of two populations with distinct morphologies was confirmed also in ultra-thin sections. Most of the crude F-actin fraction consisted of large aggregates of microfilaments intertwined with

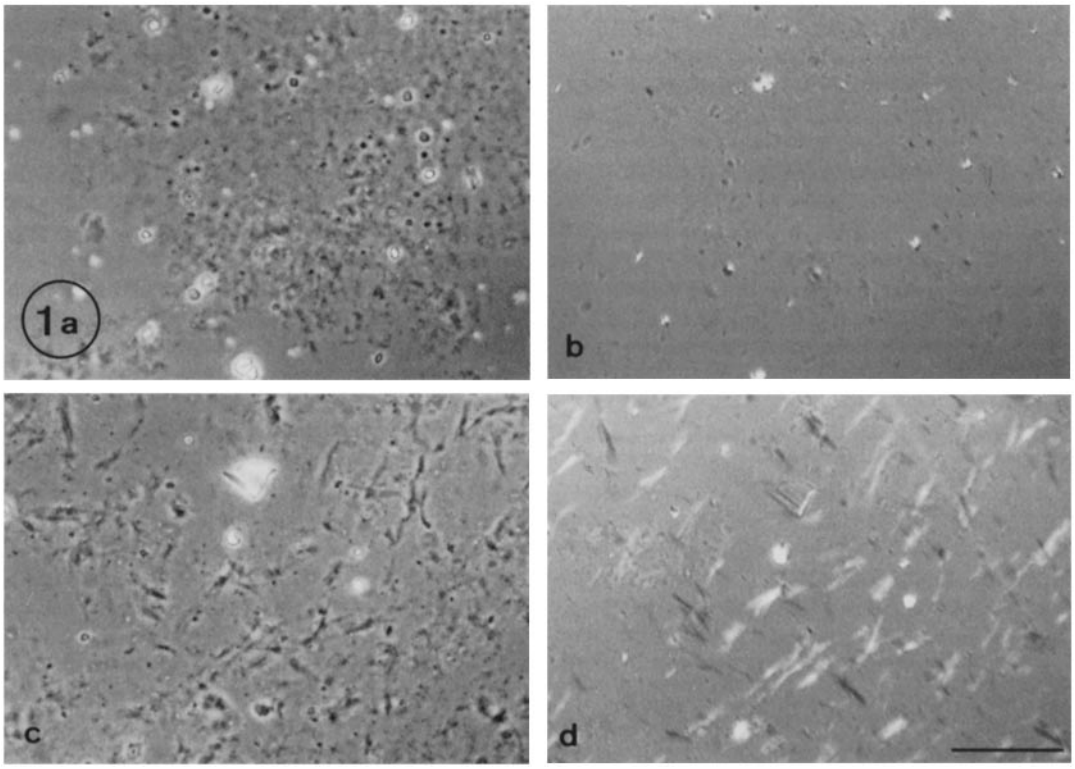

FIGURE 1 Phase-contrast and polarization micrographs of the crude F-actin fraction. Amorphous aggregates (*a*) representing most of the fraction show significant birefringence (*b*). Rod-shaped aggregates with higher phase-density (*c*) are scarce and showed strong birefringence (*d*). *a* and *b* and *c* and *d* are the same fields, respectively: (*a* and *c*) phase-contrast micrographs; (*b* and *d*), polarization micrographs. Compensator setting, +2°. Bar, 50 μm. × 300.

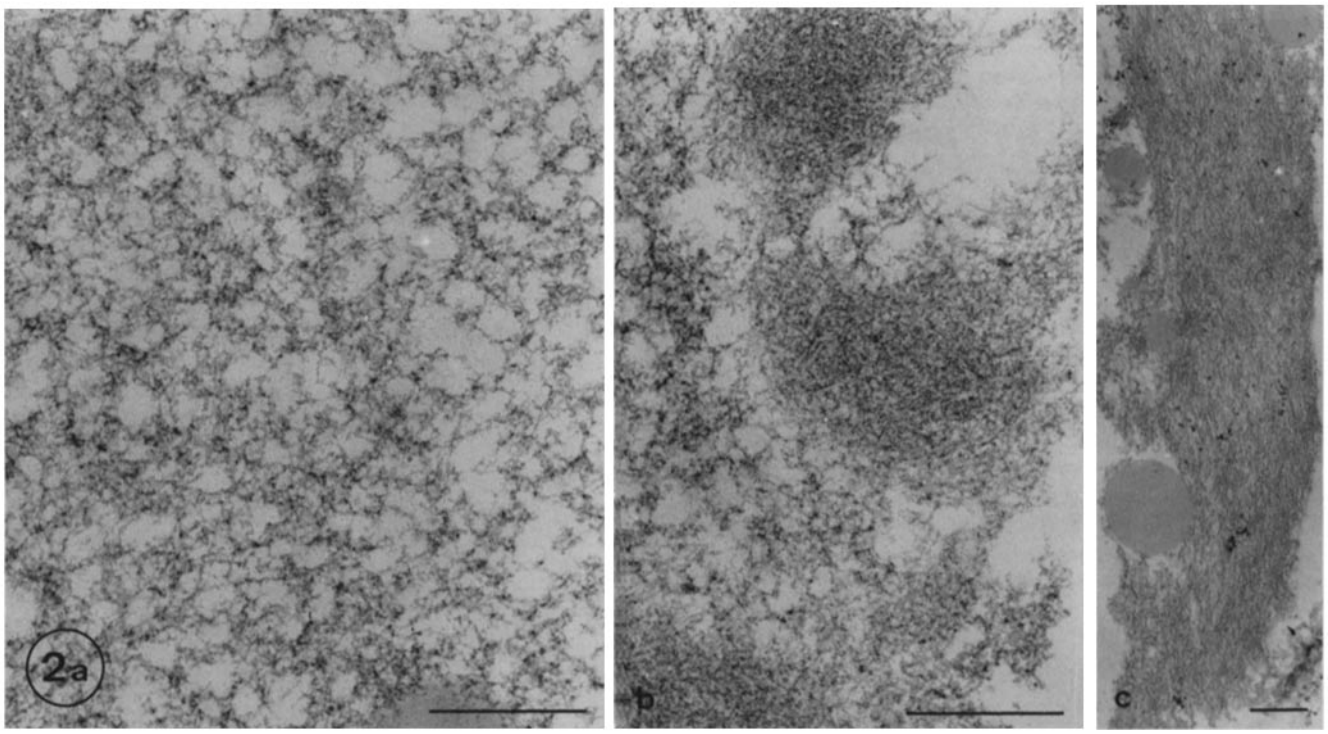

FIGURE 2 Thin sections of the crude F-actin fraction. Most of the microfilaments are entangled to form networks as in *a* and *b*. Bundles as in *c* are not frequently observed. Packing of the entangled microfilaments varied from rather loose in *a* to compact ones in *b*. Bar, 0.5 μm. (*a* and *b*) × 42,000. (*c*) × 15,000.

each other and lacking cytoplasmic organelles (Fig. 2). The morphology of the entangled microfilaments varied in compactness from rather loose (Fig. 2*a*) to extremely compact (Fig. 2*b*). The loose and the compact aggregates were often found close to each other (Fig. 2*b*). Also, large bundles of microfilaments in parallel array (Fig. 2*c*) were identified in very few

thin sections. Although quantification of the number of microfilaments in the crude F-actin fraction represented by the bundle population was difficult, the optical and electron microscopy observations indicated that the bundle population was not more than 10% of the fraction.

That the fraction was a mixture of the two microfilament populations readily distinguishable from the supramolecular arrangements does not necessarily mean that the fraction is a good cytoskeletal model. But emphasis should be laid on the identical morphologies of the entangled microfilaments and the microfilaments in the relaxation phase and of the compact bundles and the microfilaments in the contraction phase identified by electron microscopy *in situ* (20). Also, note the presence of a birefringent population which would correspond, on the basis of the dimensions and the retardation of the birefringence (27), to the in vivo fibrils appearing in the contraction phase.

The polypeptide composition of the crude F-actin fraction is given in Fig. 3. Although the gels were overloaded with the proteins, resulting in overlapping of the two major bands (42,000 and 36,000) which were clearly split in a less-loaded gel, there were unexpectedly few bands and the densitometric traces of the gel showed that ~20–30% of the fraction was represented by a polypeptide band that had the same mobility as pure plasmodial actin of 42,000 daltons, and that approximately the same amount of it was found in a 36,000-dalton polypeptide.

The actin content of the crude F-actin fraction was estimated also by the DNase inhibition assay (43). Before the assay, the fraction was well glass-homogenized, sonicated thoroughly, and then incubated in 0.75 M guanidine-HCl. The amount of the crude F-actin giving 100% inhibition of the DNase activity was 5.3 times larger than that of the pure actin, indicative of the 19% purity of the actin. This agreed with the 19% determined with the SDS PAGE densitogram of the preparation.

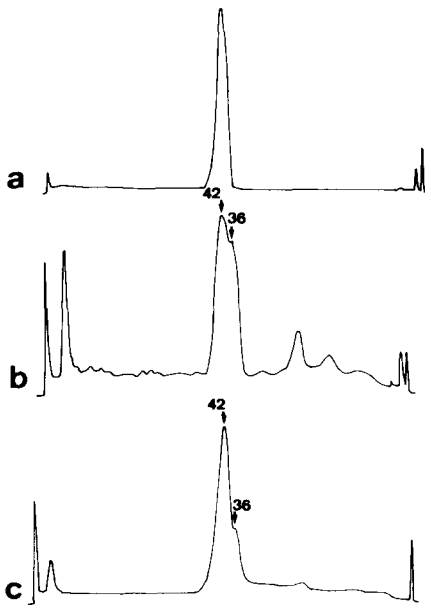

FIGURE 3 Densitometric traces of the crude F-actin fraction on SDS PAGE. In this and all electrophoresis figures, proteins were run from the left to the right in the traces. (*a*) 25 μg of plasmodial actin; (*b*) 50 μg of the crude F-actin; and (*c*) 25 μg of the crude F-actin plus 12.5 μg of plasmodial actin. Numbers × 10^3.

Examination of the Extraction Procedure for the Crude F-Actin Fraction with Respect to Possible Denaturation of Actin

To obtain the crude F-actin fraction, the plasmodia were extensively extracted in Triton X-100 and EGTA and extensively washed in EDTA and $CaCl_2$. The procedure may irreversibly denature actin by removal of ATP and bound cations, and the other chemicals in the Triton and the washing solution may have unknown effects on actin, though skeletal F-actin is known to be highly stable even if the nucleotides are removed (44) and if divalent cation chelators are added (45). We examined such a possibility by measuring HMM binding to treated and untreated plasmodial F-actins. The amount of HMM bound to F-actin was determined by measuring the increase in the light-scattering intensity at 340 nm (46), the results of which are shown in Fig. 4. Untreated actin of 0.1 mg/ml bound 0.362 mg/ml HMM. This means that ~2 mol of actin monomer bound 1 mol of HMM, and the value falls in the range of the results previously reported for skeletal actin (47). Although treatment of actin with two mixings with the Triton solution and with two washings decreased the amount of bound HMM to 0.218 mg/ml, i.e., 60% of the untreated, the control actin treated similarly not with Triton X-100, EGTA, etc., but with 50 mM KCl and 10 mM imidazole-HCl also showed a decrease in the HMM binding (0.205 mg/ml HMM, 57% of the untreated). This result clearly indicates that the decrease in the HMM binding is due to partial denaturation of actin not by the reagents used in the preparation of the crude

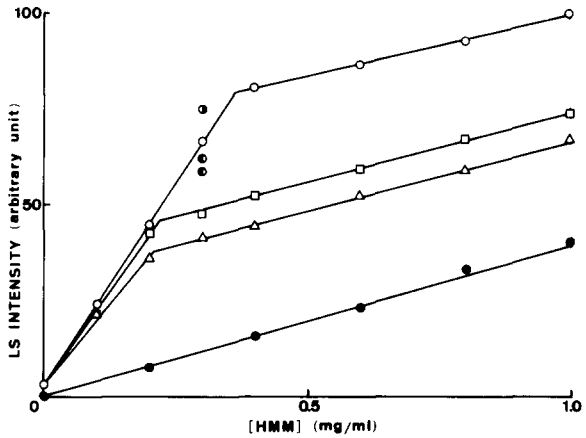

FIGURE 4 Binding of skeletal HMM to plasmodial F-actin measured by increase in the light-scattering intensity at 340 nm upon addition of various concentrations of skeletal HMM to plasmodial F-actin at a fixed concentration. Experimental conditions were 0.1 mg/ml actin, 0–1.0 mg/ml HMM, 50 mM KCl, and 20 mM imidazole-HCl, pH 7.0, 25°C. HMM alone has a light-scattering intensity depending linearly on its concentration (●). The intensity increases by the addition of F-actin and saturates at the full binding concentration of HMM. (○) HMM and untreated F-actin. (□) HMM, and F-actin treated in the same way as in the preparation of the crude F-actin fraction except that F-actin was pelleted by centrifugation at 100,000 *g* for 100 min and resuspended by glass-homogenization. (△) HMM and F-actin treated in the same way as in (□), except that the Triton solution and the washing solution were substituted for 50 mM KCl and 10 mM imidazole-HCl at pH 7.0. (◑) HMM and F-actin which was stirred for 30 min in the Triton solution at 0°C before mixing with HMM. (◐) HMM and F-actin which was stirred for 60 min in the Triton solution plus 10 mM EDTA and 10.1 mM $CaCl_2$ before mixing with HMM.

TABLE I

Apparent Purity of Actin in Crude F-Actin Fraction Estimated from Activation of ATPase Activity of Myosin and HMM Binding

	Actin/Myosin ratio at half maximal activation (g/g)		Apparent purity of actin (c)*	Actin content from SDS PAGE (d)	% of Actin interactive with myosin or HMM‡
Activation experiment	Pure F-actin (a)	Crude F-actin (b)			
	0.136	8.84	1.54%	20%	7.7%
Binding experiment	Actin/HMM binding ratio (g/g)				
	Pure F-actin (a)	Crude F-actin (b)			
	0.192	8.20	2.34%	28%	8.4%

* Calculated as (a)/(b).
‡ Calculated as (c)/(d).

F-actin fraction but rather by the repeated ultracentrifugation and glass-homogenization. F-actin that was neither ultracentrifuged nor glass-homogenized as in the crude F-actin preparation did not show any significant change in HMM binding (Fig. 4).

Unavailability of the Actin in the Crude F-Actin Fraction to Myosin

The crude F-actin fraction was examined with regard to interaction with myosin, i.e., its ability to activate the Mg-ATPase activity of myosin and to bind HMM in the absence of ATP (Table I). In both experiments, plasmodial actin almost 100% pure (Fig. 3*a*) was used as the control, and the values obtained, 0.136 of actin/myosin and 0.192 of actin/HMM weight ratio, mean an approximately 2:1 molar ratio at the saturation level. Under the same conditions, much larger values were found in the crude F-actin fraction. Comparison of the calculated apparent purity of actin in the fraction and the actin content determined by SDS PAGE densitometry indicated that >90% of the actin was masked, thus losing the ability to interact with myosin. This unavailability led us to think that a factor may exist which binds to actin, causing specific entanglement and blocking the interaction with myosin.

Purification of a Factor which Causes the Entanglement of F-Actin and Blocks Actin-Myosin Interaction

After the procedure described in Materials and Methods, the factor in question was extracted from the crude F-actin fraction and further purified to a single polypeptide by following its blocking activity of the actin-myosin interaction. Fig. 5 shows the elution profile of the active fraction in the ammonium acetate fraction. The activity was found in fractions with a peak corresponding to BSA of 68,000 daltons. However, 68,000-dalton skeletal tropomyosin, which is known to be rod-shaped, was eluted several fractions earlier than BSA. The first peak around fraction No. 18 contained mainly actin, ~200,000-dalton polypeptide, and small amounts of other proteins. The third peak around fraction No. 36 contained no protein but RNA.

Fractions No. 25–31 were pooled, passed through an activated charcoal column to remove contaminant RNA, and then rechromatographed on a smaller column of Sephacryl S-300 with the same elution buffer (Fig. 5, *inset*). They were then eluted with a single peak at 280 nm, and the ratio of 280–260 nm rose from 1.3–1.9. Table II summarizes typical yields of 36,000-dalton factor determined by its activity to inhibit the

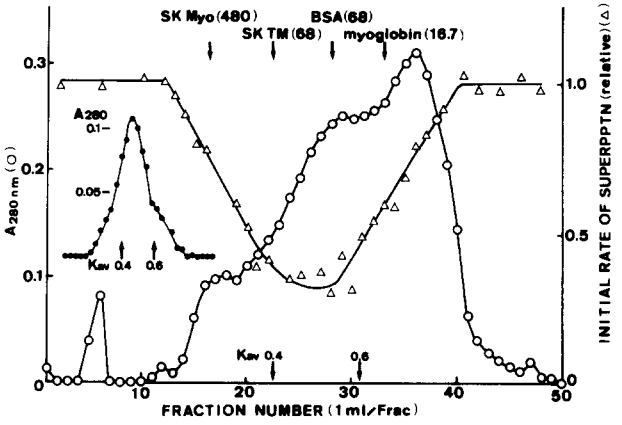

FIGURE 5 Elution profile of the active fraction in the ammonium acetate fractionation. The supernate of the 21.4% saturation (fraction II) was condensed, subjected to gel filtration on a 1.3 x 30 cm column of Sephacryl S-300 Superfine equilibrated and eluted with 0.6 M KCl, 1 mM DTT, 10 μM PMSF, and 10 mM imidazole-HCl at pH 7.0 at 2°C at a flow rate of 54 ml/h. Fractions of 1 ml were collected and assayed for the absorbance at 280 nm (○), and aliquots of the fractions were assayed for the inhibitory activity in the superprecipitation (△) by mixing with reconstituted skeletal actomyosin to give the final concentrations of 0.24 mg/ml myosin, 0.14 mg/ml F-actin, 120 mM KCl, and 10 mM imidazole-HCl buffer at pH 7.0. The reactions were started with 5 μM Mg-ATP at 21.5°C and the initial rates were determined by measuring the increase in the optical density at 660 nm. The same column was calibrated under the same conditions for the molecular weight determination with skeletal myosin (480,000 daltons), skeletal tropomyosin (68,000 daltons), bovine serum albumin (68,000 daltons) and myoglobin (16,700 daltons), and the peak fractions of the proteins are indicated by the arrows. Fractions from 25 to 31 were pooled and, after passing through an activated charcoal column, rechromatographed on a Sephacryl S-300 column. The *inset* plots (●) represent the elution profile of the second gel filtration. For details, see Materials and Methods.

superprecipitation of reconstituted skeletal actomyosin as well as by the densitometric traces of SDS PAGE of each purification step (Fig. 6). The amount of 36,000-dalton factor (arrows in Fig. 6) increased in each fraction during successive purification steps (see also Table II) and the specific activity rose in proportion to the purity of the isolation fractions, indicating the co-purification of the activity with 36,000-dalton polypeptide. The purified factor migrated as a single band on SDS PAGE (Fig. 6*e*, and *f*). Several faint broad stains were detectable in the densitometric trace when a large amount of the factor fraction was applied (30 μg, Fig. 6*f*), but they were not visible either in the gel or in the photographic reproduction.

TABLE II

Typical Yields of 36,000-dalton Factor from 100 g of Plasmodia

Stage	Total protein	Specific activity*	Total activity	Purity‡	Total§ 36,000-dalton	Yield§
	mg	*U/μg*	*U × 10⁻³*	*%*	*mg*	*%*
Total plasmodia	2,754	—	—	4.6	126	100
Crude F-actin fraction	610	—	—	6.9	42	33
Fraction I	142	0.95	135	14	20	16
Fraction II	76	1.08	82	18	14	11
Purified 36,000 dalton	9	4.39	40	96	8.3	7

* One unit is an activity of decreasing 1% of the initial rate of the superprecipitation assayed under conditions of 0.3 mg/ml skeletal myosin, 0.18 mg/ml skeletal F-actin, 50 mM KCl, 10 mM imidazole-HCl, pH 7.0, 50 μM Mg-ATP, at 25°C.

‡ Purity was determined by measuring the area corresponding to 36,000-dalton polypeptide in the densitometric traces of SDS PAGE of the fractions.

§ Total 36,000 dalton and yield were calculated based upon purity in SDS PAGE and total protein.

The molecular weight of the factor was determined by comparing the mobility in SDS PAGE with skeletal and gizzard tropomyosins as standard marker proteins, with plasmodial actin co-electrophoresed for more accuracy (Fig. 7). The molecular weight of the factor determined was ~36,000 daltons considering the precision of this analyzing system.

Fulfillment of the Criteria for the Relaxing Factor by 36,000-dalton Polypeptide

Figs. 8 and 9 show that the initial rates of the actin-activated Mg-ATPase activity and the superprecipitation of synthetic skeletal actomyosin decreased with an increasing concentration of the 36,000-dalton factor. In either case, the inhibitory activity of the 36,000-dalton factor was independent of the free Ca^{2+} concentrations in the range $\times 10^{-8}$ to $\times 10^{-3}$. In the concentration-activity plots in the inset of Fig. 9, the value extrapolated to 100% inhibition in the lower concentration range gave a weight ratio of 0.13 of factor/actin.

Another criterion for the relaxing factor, the entanglement of actin filaments, was also fulfilled by 36,000-dalton polypeptide by direct visualization of the entanglement of actin filaments in electron microscopy and by using a sedimentation assay. The factor and skeletal F-actin at 0.14 weight ratio were mixed in 0.6 M KCl and 10 mM imidazole-HCl at pH 7.0 at 2°C, and the mixture was dialyzed against 50 mM KCl and 10 mM imidazole-HCl at pH 7.0 overnight to obtain a stable complex. The mixture was then diluted appropriately with the dialyzing buffer before it was negatively stained. As seen in the low magnification micrograph (Fig. 10*a*), actin filaments were entangled by the factor, forming large aggregates reaching several tens of microns. These aggregates were often localized somewhere on an electron microscope grid while F-actin at the same concentration was dispersed freely all over the grid, with the individual filaments being rather straight. A magnified view is shown in Fig. 10*b*, where the actin filaments are heavily curled and intertwined with each other to form densely packed regions, and in some places the filaments look as though they are running in parallel with adjacent filaments, suggesting that two activities are inherent in the 36,000-dalton factor, i.e., curling and cross-linking activities. A similar result was obtained in the case of the plasmodial actin.

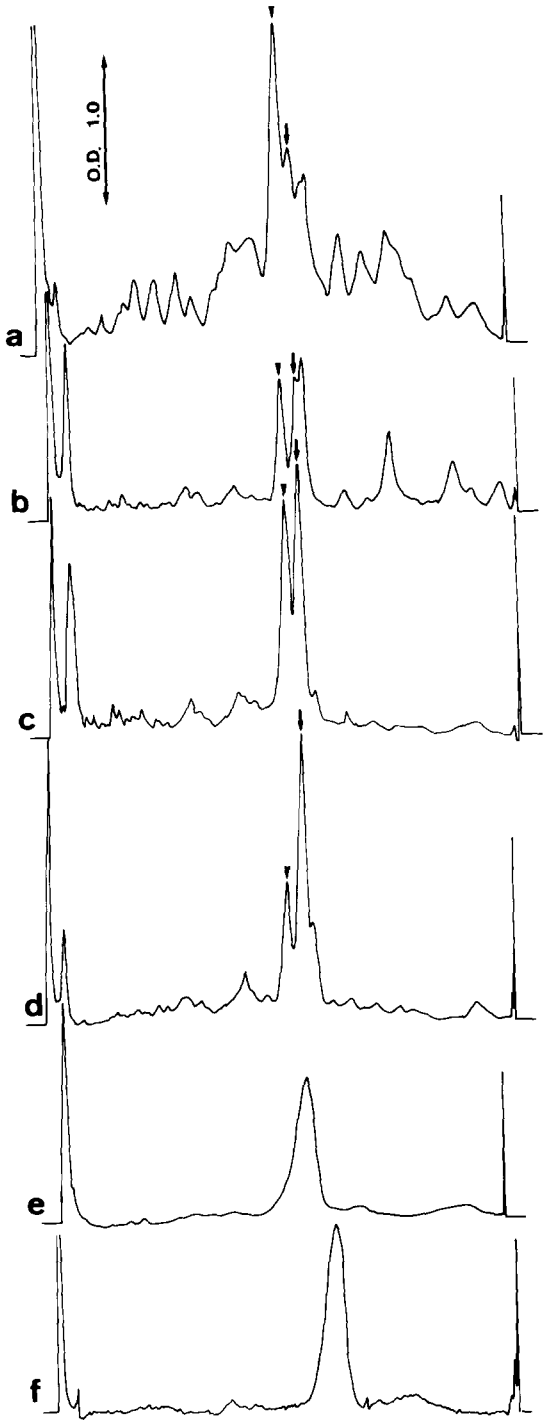

FIGURE 6 Densitometric traces of SDS PAGE analysis of 36,000-dalton factor isolation fractions. (*a*) Whole plasmodia homogenate, 25 μg. (*b*) crude F-actin fraction, 25 μg. (*c*) fraction I, 25 μg. (*d*) fraction II, 25 μg. (*e* and *f*) purified 36,000-dalton factor, 10 μg. (*e*) and 30 μg (*f*). In *f*, protein peak migrated closer to the anode side than that in *e*, due to the overloading of the sample to detect possible contaminations. Actin and 36,000-dalton factor in the successive fractions are indicated by arrowheads and arrows, respectively. Gels were scanned at 570 nm, and the optical density is shown by the scale of 1.0.

Assuming that these large aggregates of the complex would sediment much faster than dispersed actin filaments, we tested to see whether the sedimentation of actin was enhanced by the factor. Fig. 11*a* shows that the 36,000-dalton factor made F-

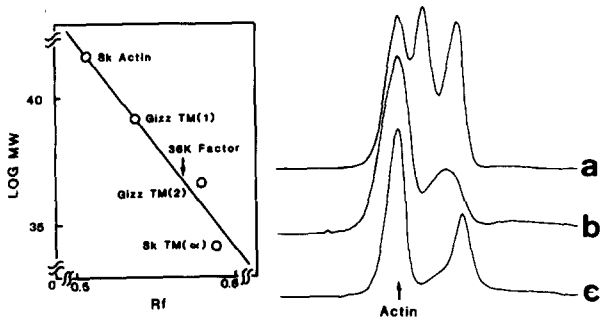

FIGURE 7 SDS PAGE analysis of the molecular weight of 36,000 factor. Electrophoresis was performed as described in Fig. 3. Densitometric traces: (*a*) 5 μg plasmodial actin plus 10 μg chicken gizzard tropomyosin; (*b*) 5 μg plasmodial actin plus 5 μg 36,000-dalton factor; and (*c*) 5 μg plasmodial actin plus 5 μg skeletal tropomyosin. The *Rf* values of each protein were calculated with coelectrophoresed actin as a common *Rf* value for accuracy. Under the conditions of loading a small amount of the samples on 7.5% polyacrylamide gels, two polypeptides of gizzard tropomyosin split clearly and only the α-chain of skeletal tropomyosin was seen as a distinct peak. Molecular weight of each protein was: actin, 42,000; gizzard tropomyosin, 39,000, and 36,000 (71); α-chain of skeletal tropomyosin, 34,000.

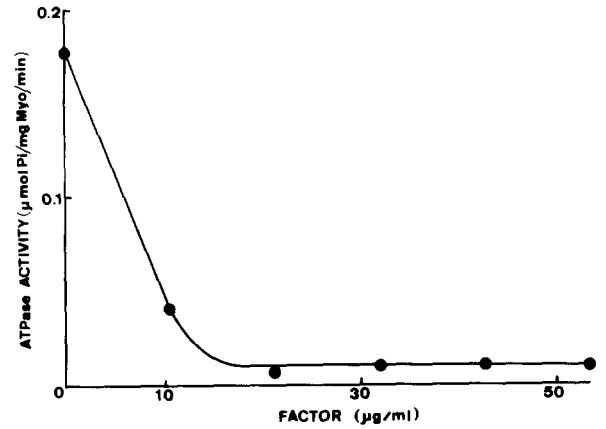

FIGURE 8 Inhibition by 36,000-dalton factor of the actin-activated Mg-ATPase activity of skeletal myosin. The assay conditions were 50 μg/ml myosin, 8.4 μg/ml skeletal F-actin, 50 μM ATP, 2 mM $MgCl_2$, 50 mM KCl, and 20 mM imidazole-HCl buffer at pH 7.0. The ATPase activity in the initial 45 s at 20°C is plotted against the concentrations of 36,000-dalton factor.

actin become much more sedimentable than F-actin alone. Without 36,000-dalton factor, F-actin sedimented so slowly that centrifugation for more than 1.5 h at 78,000 *g* was needed for full sedimentation. In contrast, the 36,000-dalton factor-actin complex almost fully sedimented within 45 min by the same centrifugal force. As seen in the short-time centrifugation within 45 min, the complex sedimented about 8 times faster than F-actin alone, even when only 0.23 μg of the factor was added to 14.5 μg of actin, i.e., 0.016 of factor/actin weight ratio, which was much smaller than that suggested by the foregoing result of the superprecipitation assay (0.13; Fig. 9, *inset*).

Direct binding of the 36,000-dalton factor to skeletal actin was tested. Actin was combined with 36,000-dalton factor at the weight ratio of 0.3 of factor/actin. The 36,000-dalton factor was clarified at 78,000 *g* for 45 min before mixing, and only bound 36,000-dalton factor would be pelleted with actin. The mixture was centrifuged at 78,000 *g* for 45 min, where the

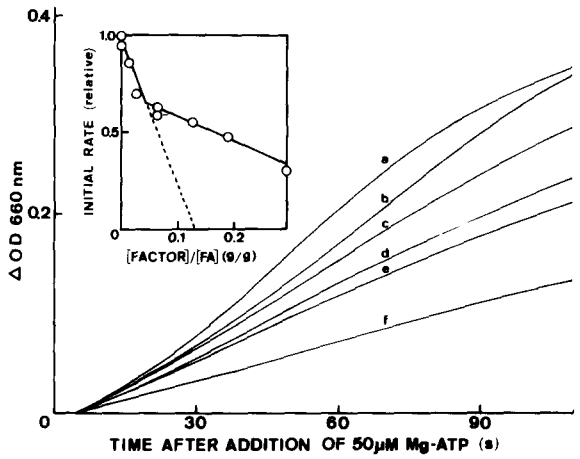

FIGURE 9 Inhibition of the superprecipitation of synthetic skeletal actomyosin by 36,000 factor. The assay conditions were similar to those described in Fig. 5. The reaction mixture contained 0.24 mg/ml myosin, 0.15 mg/ml F-actin, 113 mM KCl, 0.2 mM DTT, 2 μM PMSF, and 10 mM imidazole-HCl buffer at pH 7.0 at 25°C, plus 36,000-dalton factor at the concentrations (μg/ml): (*a*) 0; (*b*) 1.9; (*c*) 3.8; (*d*) 9.6; (*e*) 29; and (*f*) 45. The *inset* shows the dependence of the initial rates on the amount of the factor (*FACTOR/FA*; weight ratio of 36,000-dalton factor to F-actin).

complex was pelleted completely while actin was pelleted only slightly (Fig. 11*a*), and the pellet was analyzed. From the densitometric trace (Fig. 11*b*), the 36,000-dalton factor/actin weight ratio was determined and the value was found 0.12. If we take into consideration that, under the centrifugation conditions employed, 14% of actin was pelleted without 36,000-dalton factor (Fig. 11*a*), the weight ratio is corrected as 0.14. However, the enhancement of the sedimentability of actin by 36,000-dalton factor was very great even when a small amount of 36,000-dalton factor was combined (Fig. 11*a*), suggesting that most of the actin was not free but combined in large aggregates under the conditions in Fig. 11*b*. This implies that the binding weight ratio is much smaller than 0.14 and slightly larger than 0.12, which is consistent with the value predicted in the superprecipitation assay (0.13; Fig. 9, *inset*).

Comparison of 36,000-dalton Factor with Tropomyosin

The polypeptide molecular weight of 36,000-dalton factor in SDS PAGE is very close to that of tropomyosins (Fig. 7). The factor binds to F-actin and modifies the actin-myosin interaction. Also, its activity was found, in a separate experiment, in a fraction of 60–80% saturated ammonium sulfate (data not shown). These facts seemed to suggest that the 36,000-dalton factor might be very close in nature to tropomyosin but comparison of them proved this to be unlikely. (*a*) In the ultraviolet spectra, the maximum absorbance of 36,000-dalton factor at 278 nm was 3.6 times larger than that of skeletal tropomyosin. (*b*) The amino acid compositions of 36,000-dalton factor and skeletal tropomyosin shown in Table III suggest that the two are different. Note the abundant presence of proline, tyrosine and phenylalanine in the 36,000-dalton factor, the latter two explaining the larger absorbance in the UV spectrum. (*c*) The 36,000-dalton factor did not form paracrystalline aggregates in either 50 mM $MgCl_2$ or $CaCl_2$ unlike in the case of skeletal and smooth tropomyosin (48). (*d*) In electron microscopy, no entanglement of actin filaments was seen in the case of skeletal

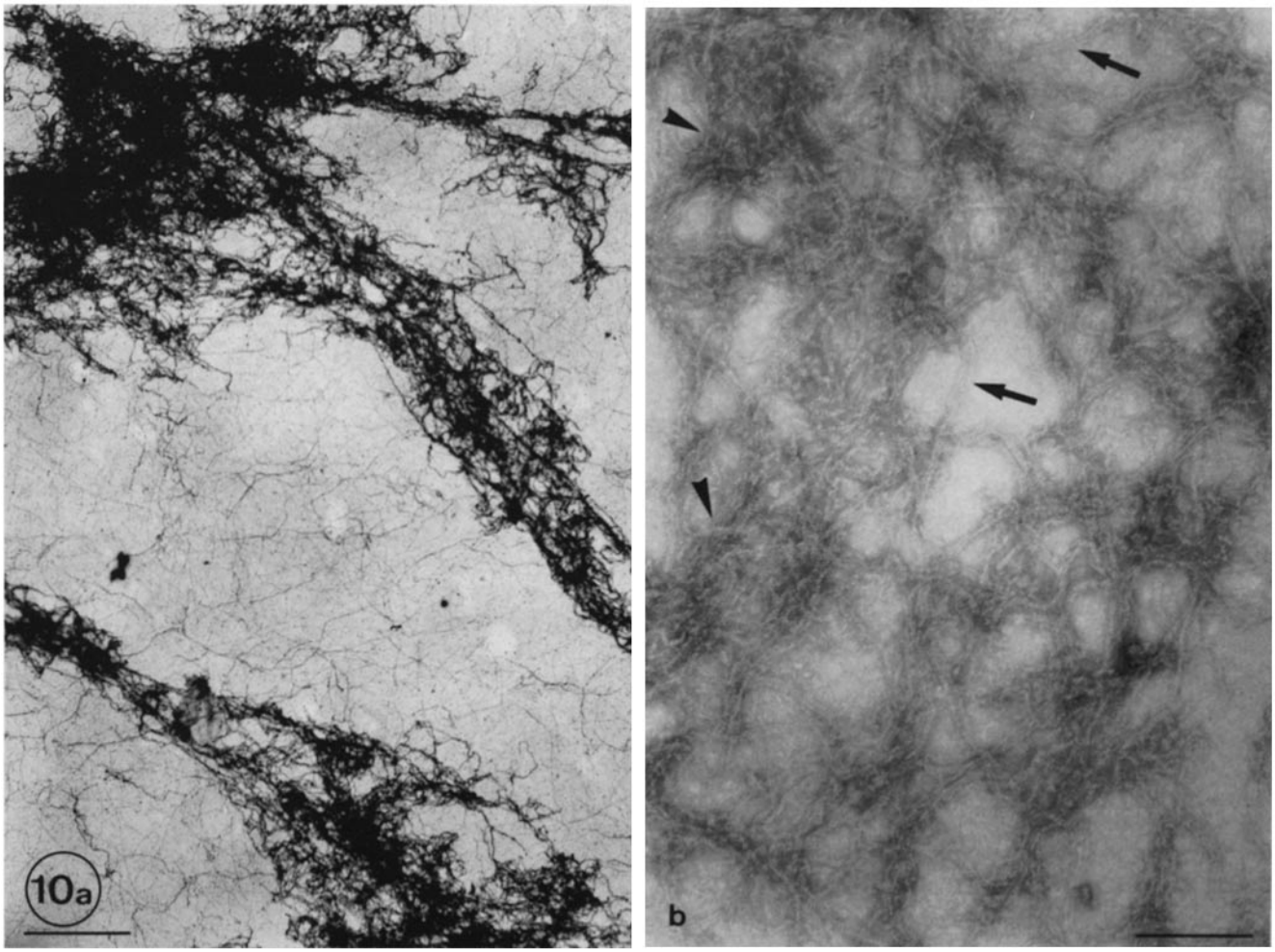

FIGURE 10 Electron micrograph of a negatively stained complex of actin filaments and 36,000-dalton factor. 36,000-dalton factor and skeletal F-actin at the weight ratio of 0.14 were mixed in 0.6 M KCl and 10 mM imidazole-HCl at pH 7.0 at 2°C and dialyzed overnight against 50 mM KCl and 10 mM imidazole-HCl at pH 7.0 (*a*). (*b*) A higher magnification of the same specimen as *a*. Note that the actin filaments run in parallel with adjacent filaments (arrows), and also note that they are heavily curled and intertwined with each other to form densely packed regions (arrowheads). (*a*) Bar, 0.5 μm; × 28,000. (*b*) Bar, 0.2 μm; × 32,000.

tropomyosin at the weight ratio of 0.23 to actin under conditions similar to those described in Fig. 11. (*e*) Under conditions similar to those for the 36,000-dalton factor (Fig. 9; 0.24 mg/ml skeletal myosin, 0.15 mg/ml skeletal F-actin, and 50 μM Mg-ATP), skeletal tropomyosin enhanced the rates of the superprecipitation in proportion to its concentrations to give a full activation when 0.23 ratio of F-actin was added, as previously reported (49). (*f*) Binding of skeletal troponin to the 36,000-dalton factor was tested (Table IV). F-actin, F-actin plus skeletal tropomyosin, and F-actin plus 36,000-dalton factor were almost completely pelleted with centrifugation at 100,000 *g* for 2 h. Note that the complex of F-actin and 36,000-dalton factor was more sedimentable than F-actin alone, supporting the data in Fig. 10*a*. As was reported previously (50), troponin loosely bound to F-actin (26.1%) but formed a more tight complex when tropomyosin was present (98.0%). In contrast, troponin hardly bound to a F-actin–36,000-dalton factor complex; the troponin binding to complex (25.8%) was not more than that found in the combination of troponin and F-actin. These data clearly show that skeletal troponin did not bind to the 36,000-dalton factor and indicate that the 36,000-dalton factor is distinct from tropomyosin.

DISCUSSION

Demembranation and extensive washing of the plasmodia with Triton X-100, EGTA, and EDTA yielded a cytoskeletal preparation, the crude F-actin fraction, consisting mostly of entangled microfilaments closely resembling the microfilament morphology in the relaxing phase of living plasmodia (Figs. 1 and 2). Inclusion in this fraction of a small amount of microfilament bundles that closely resembled the bundles found in the contracting plasmodia (Fig. 1 and 2), as well as the examination of possible effects of the isolation procedure on actin denaturation (Fig. 4), assures that the demembranating conditions employed here yielded well-conserved microfilament populations observed in electron microscopy in vivo (20). The very small probability of a bundle population's being present in the fraction suggests that the fractionation condition favor the stabilization of the relaxed state of the plasmodia. Examination of the ability of the fraction to interact with myosin showed that >90% of the actin was not available to myosin (Table I). Furthermore, the fraction contained unexpectedly few polypeptides (Figs. 3*b* and 6*b*). Encouraged by these findings, we focused on the protein that remained strongly associated with

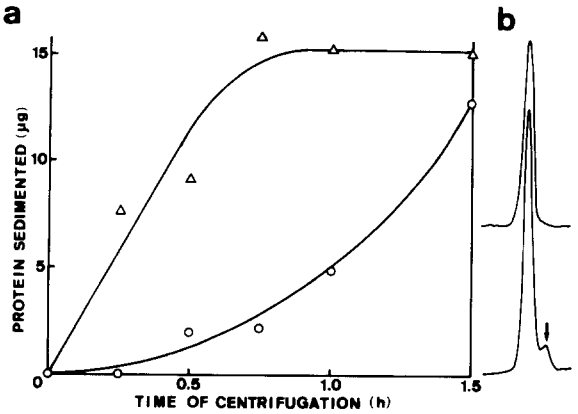

FIGURE 11 (*a*) Enhancement of sedimentability of F-actin by 36,000-dalton factor and (*b*) the direct binding stoichiometry. (*a*) Before experiments, 36,000-dalton factor was centrifuged at 78,000 *g* for 45 min to remove aggregated material. In centrifuge tubes, 14.5 μg skeletal F-actin was mixed with (Δ) or without (○) 0.23 μg 36,000-dalton factor in total volume of 0.5 ml of 50 mM KCl, 0.5 mM β-ME, 10 μM PMSF and 10 mM imidazole-HCl at pH 7.0 on ice. The tubes were then spun at 78,000 *g* for 15 min to 1.5 h at 4°C. The supernates were removed and the pellets were assayed for protein concentrations by the method of Lowry (40). (*b*) Densitometric traces of SDS PAGE of the pelleted 36,000-dalton-actin complex. 30 μg/ml skeletal F-actin was mixed with 9 μg/ml 36,000-dalton factor in the same buffer as above, and the mixture was then spun at 78,000 *g* for 45 min. The supernate was removed and the pellet was solubilized with 2% SDS and subjected to SDS PAGE. Upper trace shows actin used and lower trace shows the sedimented complex. Gels were stained and scanned as described in Materials and Methods. Relative amounts of stained materials were determined by cutting out and weighing relevant peaks. Arrow indicates 36,000-dalton factor.

TABLE III

Amino Acid Compositions of 36,000-dalton Factor and Skeletal Tropomyosin

	36,000-dalton factor	Tropomyosin*
Asp	11.9	10.7
Thr	6.1	1.0
Ser	8.2	4.7
Glu	12.7	25.0
Pro	4.7	0.2
Gly	9.2	1.5
Ala	7.9	12.7
Val	7.1	3.3
Met	1.2	2.0
Ile	4.8	4.0
Leu	8.1	11.3
Tyr	2.8	0
Phe	4.5	0.5
Lys	5.6	13.2
His	2.0	0.7
Arg	3.3	5.2
Try	ND	1.8
Cys	ND	1.5

Compositions are expressed as mole %. *ND*, not determined.
* See Reference 71.

F-actin during the exhaustive demembranation and washing out of the cytoplasmic inclusions, and we found that a single polypeptide, 36,000-dalton polypeptide, isolated and purified from the fraction, relaxed actin filaments by entangling them and blocking the interaction with myosin.

The 36,000-dalton factor binds to F-actin in a 0.12–0.14 weight ratio as was demonstrated in the direct binding assay

TABLE IV

Interaction of Troponin with F-Actin-Tropomyosin and with F-Actin-36,000-dalton Complexes

Components added	Protein in supernates	Bound TN
	mg/ml	%
FA	0.031	—
FA + TM	0.033	—
FA + 36 K	0.020	—
FA + TN	0.216	26.1*
FA + TM + TN	0.039	98.0‡
FA + 36,000 dalton + TN	0.205	25.8§

Protein concentrations were: 1.39 mg/ml skeletal F-actin (*FA*), 0.25 mg/ml skeletal tropomyosin (*TM*), 0.126 mg/ml 36,000-dalton factor, 0.25 mg/ml skeletal troponin (*TN*). Before experiments, tropomyosin, 36,000-dalton factor and troponin in 150 mM KCl and 10 mM imidazole-HCl at pH 7.0 were centrifuged at 100,000 *g* for 2 h at 4°C. Proteins were mixed in 150 mM KCl, 2 mM $MgCl_2$, and 10 mM imidazole-HCl at pH 7.0 on ice, and the mixtures were centrifuged at 100,000 *g* for 2 h at 4°C. The supernates were assayed for the protein concentrations by microbiuret method (42).

* $\left\{1 - \frac{(FA + TN) - (FA)}{0.25}\right\} \times 100.$

‡ $\left\{1 - \frac{(FA + TM + TN) - (FA + TM)}{0.25}\right\} \times 100.$

§ $1 - \left\{\frac{(FA + 36{,}000\ dalton + TN) - (FA + 36{,}000\ dalton)}{0.25}\right\} \times 100.$

(Fig. 10*b*). This value was consistent with that predicted in the superprecipitation assay, i.e., 0.13 (Fig. 9). In the concentration-activity plots in the latter assay system, however, a distinct break was found. The extrapolated value in a higher concentration range to 100% inhibition gives the weight ratio of 0.57 factor/actin. Also, the weight ratio estimated from the Mg-ATPase assay gives a much greater value (1.55, Fig. 8), and this was the case also in the crude fractions during purification; the factor/actin ratios were always about ten times larger in the Mg-ATPase assay than in the superprecipitation assay. These two larger values (0.57 and 1.55) may reflect the high content of 36,000-dalton factor in the plasmodia and in the crude F-actin fraction (Fig. 6*a* and *b*), but the physiological significance of the larger values is not known. The value 0.13 gives the binding molar ratio of 6.6 mol of actin per mol of 36,000-dalton factor. Assuming that the factor is a globular dimer of 72,000 daltons in the native protein, as was suggested by the finding that 36,000-dalton factor was eluted in the gel filtration around the peak fraction of 68,000-dalton BSA (Fig. 5), 1 mol of the factor binds to 13 mol of actin, half a helix. However, we cannot exclude the possibility that the 36,000-dalton factor may be a very asymmetric protein of 36,000-dalton, judging from Fig. 5, until more is known about this protein.

Although the 36,000-dalton factor identified in this study inhibited and skeletal tropomyosin activated the initial rates of superprecipitation of actomyosin reconstituted from skeletal myosin and skeletal actin under similar conditions (50 μM ATP), these opposing actions do not necessarily lead us to conclude that the two are different, because such opposing effects have been reported in smooth and skeletal tropomyosins (51). Also, differences in the molecular weight between skeletal and nonmuscle tropomyosins from vertebrate sources (52–54) would not rule out homology between 36,000-dalton factor to tropomyosin. Comparing the amino acid compositions of skeletal and nonmuscle tropomyosins (53, 54) with that of the 36,000-dalton factor (Table III), however, the abundant presence of proline and of two hydrophobic amino acids, tyrosine

and phenylalanine, in the 36,000-dalton factor strongly suggests that the structure of this protein is much different from that of rod-shaped tropomyosin of alpha helices. Furthermore, skeletal tropomyosin did not make actin filaments become entangled, unlike the 36,000-dalton factor; the entangled complex of the 36,000-dalton factor and actin filaments (Fig. 10) was prepared by dialyzing overnight the mixture of the two in 0.6 M KCl at the weight ratio demonstrated by the direct binding assay (Fig. 11 *b*) against 50 mM KCl, thus eliminating a possibility that the entanglement of actin filaments, as shown in Fig. 10, might represent a transient state of the complex under nonequilibrium conditions. Finally, we presented a result that the skeletal troponin did not bind to 36,000-dalton factor under the conditions where it fully bound to skeletal tropomyosin-actin complex (Table IV). Several tropomyosins from nonmuscle sources are reported to form calcium-sensitive hybrids with skeletal troponin (53, 54). Therefore, the failure of the troponin binding to 36,000-dalton factor serves as crucial evidence for the view that the 36,000-dalton factor is distinct from tropomyosin. In this context, the regulation of the motility of the plasmodia by Ca ions (55, 56, 57, 58, 73) is intriguing. A previous preliminary study of "tropomyosin-troponin complex" isolated from the plasmodia showed its dramatic control over synthetic skeletal actomyosin in a Ca^{2+}-sensitive fashion (59). On the basis of its function being linked with actin and of the presence of polypeptide bands in SDS PAGE similar to those of skeletal native tropomyosin, the crude complex was concluded to be similar to skeletal tropomyosin-troponin complex, despite the apparent absence of a polypeptide corresponding to troponin C. Since we have not been successful so far in isolating tropomyosin from the plasmodia in spite of the above report, which hence does not enable us to perform a detailed comparison between the 36,000-dalton factor and plasmodial tropomyosin, we can not deny the possibility of the similarity between "plasmodial tropomyosin" in the "tropomyosin-troponin complex" and tropomyosin. Nevertheless, if we assume that the 36,000-dalton factor corresponds to the "tropomyosin" polypeptide band in SDS PAGE of their preparation (~35,000-daltons), then the motility of the plasmodia is to be regulated in a way much different from that of skeletal muscle where the tropomyosin-troponin complex plays an important role. The absence of a Ca^{2+}-sensitivity in the 36,000-dalton factor implies a requirement of some other factor(s) conferring a Ca^{2+}-sensitivity in the control of contractility of actomyosin by the 36,000-dalton factor. Such unknown factors might be present in the "tropomyosin-troponin complex" (59) as "troponin."

Filamin from smooth muscles or a high molecular weight protein (HMWP) from nonmuscle cells induces actin gel by cross-linking actin filaments, and the gelled materials have some consistency. In the gel, actin filaments are in meshwork forms (60) or sometimes in regularly spaced, ladderlike structures (61). Filamin from chicken gizzard is also reported to inhibit the actin-activated ATPase activity of myosin (62, 63). Note that the actin filaments that were entangled by the 36,000-dalton factor adhere to adjacent filaments in some places to form a parallel array (Fig. 10 *b*), thus suggesting the factor's cross-linking activity other than its activity to curl actin filaments. The amino acid composition of the 36,000-dalton factor (Table III) seems close to that of filamin or HMWP (61, 64, 65, 66), so that we do not think it impossible that the 36,000-dalton factor is one of such a repetitive domain in filamin or HMWP as is known in tropomyosin (67) and calcium-binding proteins (68); the polypeptide molecular weight of filamin or HMWP (220,000–250,000) is six to seven times larger than that of the 36,000-dalton factor, and their amino acid sequences may have a several-times repeated substructure which is common to 36,000-dalton factor.

It is intriguing that the large aggregates in the network form of entangled actin filaments (Fig. 1) had some consistency as was described in Results. Although further studies are needed before we can establish the physiological significance of the interaction between the 36,000-dalton factor and actin for the contraction-relaxation cycles in plasmodia, speculating that the condition of the consistency contributes to the structural maintenance in the gel layer of the living plasmodia is very attractive as a structural apparatus constructed of entangled microfilaments consisting of actin and 36,000-dalton factor (and some other factors) is also mobilized as a contractile apparatus by changing its arrangement into parallel bundles. Just before contraction occurs, release of 36,000-dalton factor from actin filaments, which apparently means an increased availability of F-actin to myosin, would enable the formation of the actin-myosin complex in a parallel arrangement, which readily leads to the generation of motive force (69, 70). Thus, the 36,000-dalton factor is not only a possible candidate for the construction of the cytoskeleton through formation of large aggregates of actin filaments but is also a potential modifier of the actin-myosin interaction, working bifunctionally in both the cytoskeletal and the contractile aspects of the plasmodia.

The authors are grateful to Dr. Y. Fukui of our department for his kind endeavors in reading the manuscript.

This investigation was supported by grants from the Ministry of Education, Science and Culture of Japan, and from the Muscular Dystrophy Association, Inc.

Received for publication 23 April 1981, and in revised form 22 October 1981.

REFERENCES

1. Pollard, T. D., and R. R. Weihing. 1974. Actin and myosin in cell movement. *Crit. Rev. Biochem.* 2:1–65.
2. Goldman, R. D., A. Milsted, J. A. Schloss, J. Starger, and M.-J. Yerna. 1979. Cytoplasmic fibers in mammalian cells: cytoskeletal and contractile elements. *Annu. Rev. Physiol.* 41:703–722.
3. Buckley, I. K., and K. R. Porter. 1967. Cytoplasmic fibrils in living cultured cells: a light and electron microscope study. *Protoplasma.* 64:349–380.
4. Goldman, R. D., J. A. Schloss, and J. M. Starger. 1976. Organizational changes of actinlike microfilaments during animal cell movement. *In* Cell Motility. R. Goldman, T. Pollard, and J. Rosenbaum, editors. Cold Spring Harbor Laboratory, Cold Spring Harbor, New York. 217–247.
5. Tilney, L. G., and M. S. Mooseker. 1971. Actin in the brush border of epithelial cells of the chicken intestine. *Proc. Natl. Acad. Sci. U. S. A.* 68:2166–2615.
6. Burgess, R. D., and T. E. Schroeder. 1977. Polarized bundles of actin filaments within microvilli of fertilized sea urchin eggs. *J. Cell Biol.* 74:1032–1037.
7. Edds, K. T. 1977. Dynamic aspects of filopodial formation by reorganization of microfilaments. *J. Cell Biol.* 73:479–491.
8. Schroeder, T. E. 1973. Actin in dividing cells: contractile ring filaments bind heavy meromyosin. *Proc. Natl. Acad. Sci. U. S. A.* 70:1688–1692.
9. Nagai, R., and L. I. Rebhun. 1966. Cytoplasmic microfilaments in streaming *Nitella* cells. *J. Ultrastruct. Res.* 14:571–589.
10. Reaven, E. P., and S. G. Axline. 1973. Subplasmalemmal microfilaments and microtubules in resting and phagocytizing cultivated macrophages. *J. Cell Biol.* 59:12–27.
11. Spooner, B. S., K. M. Yamada, and N. K. Wessells. 1971. Microfilaments and cell locomotion. *J. Cell Biol.* 49:595–613.
12. Bryan, J., and R. E. Kane. 1978. Separation and interaction of the major components of sea urchin actin gel. *J. Mol. Biol.* 125:207–224.
13. Stossel, T. P., and J. H. Hartwig. 1975. Interactions between actin, myosin, and an actin-binding protein from rabbit alveolar macrophages. *J. Biol. Chem.* 250:5706–5712.
14. Shizuta, Y., H. Shizuta, M. Galls, P. Davies, and I. Pastan. 1976. Purification and properties of filamin, an actin binding protein from chicken gizzard. *J. Biol. Chem.* 21:6562–6567.
15. Wang, K., J. F. Ash, and J. Singer. 1975. Filamin, a new high-molecular-weight protein found in smooth muscle and non-muscle cells. *Proc. Natl. Acad. Sci. U. S. A.* 72:4483–4486.
16. Bretscher, A., and K. Weber. 1979. Villin: the major microfilament-associated protein of the intestinal microvillus. *Proc. Natl. Acad. Sci. U. S. A.* 76:2321–2325.
17. Mimura, N., and A. Asano. 1979. Ca^{2+}-sensitive gelation of actin filaments by a new protein factor. *Nature (Lond.).* 282:44–48.
18. Pollard, T. D., J. Levy, G. Isenberg, and U. Abei. 1980. Two new *Acanthamoeba* proteins

involved with regulation of actin filament cross-linking. *J. Cell Biol.* 87(2, Pt. 2):223*a* (Abstr.).
19. Bretscher, A., and K. Weber. 1980. Fimbrin, a new microfilament-associated protein present in microvilli and other cell surface structures. *J. Cell Biol.* 86:335–340.
20. Nagai, R., Y. Yoshimoto, and N. Kamiya. 1978. Cyclic production of tension force in the plasmodial strand of *Physarum polycephalum* and its relation to microfilament morphology. *J. Cell Sci.* 33:205–225.
21. Wohlfarth-Bottermann, K. E. 1964. Cell structure and their significance for ameboid movement. *Int. Rev. Cytol.* 16:61–132.
22. Condeelis, J. S., and D. L. Taylor. 1977. The contractile basis of ameboid movement V: the control of gelation, solation, and contraction in extracts from *Dictyostelium discoideum*. *J. Cell Biol.* 74:901–927.
23. Hellewell, S., and D. L. Taylor. 1979. The contractile basis of ameboid movement VI: the solation-contraction hypothesis. *J. Cell Biol.* 83:633–648.
24. Wohlfarth-Bottermann, K. E. 1962. Weitreichende, fibrillare Protoplasmadifferenzierungen und ihre Bedeutung für die Protoplasma strömung II: Lichtmikroscopische Darstellung. *Protoplasma.* 54:514–539.
25. Nakajima, H., and R. D. Allen. 1965. The changing pattern of birefringence in plasmodia of the slime mold, *Physarum polycephalum*. *J. Cell Biol.* 25:361–374.
26. Kamiya, N. 1973. Contractile characteristics of the myxomycete plasmodium. *In:* Proceedings of the IV International Biophysics Congress. G. Frank, editor. Moscow. 447–494.
27. Ogihara, S., and K. Kuroda. 1979. Identification of a birefringent structure which appears and disappears in accordance with the shuttle streaming in *Physarum* plasmodia. *Protoplasma.* 100:167–177.
28. Camp, W. G. 1936. A method of cultivating myxomycete plasmodia. *Bull. Torrey Bot. Club.* 63:205–210.
29. Perry, S. V. 1955. Myosin adenosinetriphosphatase. *Methods Enzymol.* 2:582–588.
30. Szent-Györgyi, A. G. 1953. Meromyosins, the subunits of myosin. *Arch. Biochim. Biophys.* 42:305–320.
31. Spudich, J. A., and S. Watt. 1971. The regulation of rabbit skeletal muscle contraction. *J. Biol. Chem.* 246:4866–4871.
32. Ebashi, S., and F. Ebashi. 1964. A new protein component participating in the superprecipitation of myosin B. *J. Biochem.* (*Tokyo*). 55:604–613.
33. Ebashi, S., T. Wakabayashi, and F. Ebashi. 1971. Troponin and its components. *J. Biochem.* (*Tokyo*) 69:441–445.
34. Ebashi, S., A. Kodama, and F. Ebashi. 1968. Troponin I: preparation and physiological function. *J. Biochem.* (*Tokyo*) 64:465–477.
35. Hatano, S., and K. Owaribe. 1977. A simple method of the isolation of actin from myxomycete plasmodia. *J. Biochem.* (*Tokyo*) 82:201–205.
36. Martin, J. B., and D. M. Doty. 1949. Determination of inorganic phosphate: modification of isobutyl alcohol procedure. *Anal. Chem.* 21:965–967.
37. Weber, K., and M. Osborn. 1969. The reliability of molecular weight determinations by dodecyl sulfate-polyacrylamide gel electrophoresis. *J. Biol. Chem.* 244:4406–4412.
38. Hayashi, Y. 1972. Submolecular structure of subfragment-1 of the myosin molecule. *J. Biochem.* (*Tokyo*). 72:83–100.
39. Gornall, A. G., C. J. Bardawill, and M. M. David. 1949. Determination of serum proteins by means of the biuret reaction. *J. Biol. Chem.* 177:751–766.
40. Lowry, O. H., N. J. Rosebrough, A. L. Farr, and R. J. Randall. 1951. Protein measurement with the Folin phenol reagent. *J. Biol. Chem.* 193:265–275.
41. Bensadaun, A., and D. Weinstein. 1976. Assay of proteins in the presence of interfering materials. *Anal. Biochem.* 70:241–250.
42. Itzhaki, R. F., and D. M. Gill. 1964. A micro-biuret method for estimating proteins. *Anal. Biochem.* 9:401–410.
43. Blikstad, I., F. Mareky, L. Carlsson, T. Persson, and U. Lindberg. 1878. Selective assay of monomeric and filamentous actin in cell extracts, using inhibition of deoxyribonuclease I. *Cell.* 15:935–943.
44. Mommaerts, W. F. H. M. 1952. The molecular transformations of actin III: the participation of nucleotides. *J. Biol. Chem.* 198:469–475.
45. Tonomura, Y., and J. Yoshimura. 1961. Removal of bound nucleotide and calcium of G-actin by treatment with ethylenediaminetetraacetic acid. *J. Biochem.* (*Tokyo*) 50:79–80.
46. Tonomura, Y., S. Tokura, and K. Sekiya. 1962. Binding of myosin A to F-actin. *J. Biol. Chem.* 237:1074–1081.
47. Takeuchi, K., and Y. Tonomura. 1971. Formation of acto-H-meromyosin and acto-subfragment-1 complexes and their dissociation by adenosine triphosphate. *J. Biochem.* (*Tokyo*) 70:1011–1026.
48. Takeuchi, K., and Y. Tonomura. 1977. Kinetic and regulatory properties of myosin adenosine triphosphatase purified from arterial smooth muscle. *J. Biochem.* (*Tokyo*) 82:813–833.
49. Martonosi, A. 1962. Studies on actin. *J. Biol. Chem.* 237:2795–2803.
50. Shigekawa, M., and Y. Tonomura. 1972. Active subfragment of the inhibitory component of troponin. *J. Biochem.* (*Tokyo*). 72:957–971.
51. Sobieszek, A., and S. Small. 1981. Effect of muscle and non-muscle tropomyosin in reconstituted skeletal muscle actomyosin. *Eur. J. Biochem.* 118:533–539.
52. Fine, R. E., A. L. Blitz, S. E. Hitchcock, and B. Kaminer. 1973. Tropomyosin in brain and growing neurones. *Nature New Biol.* 245:182–186.
53. Fine, R. E., and A. L. Blitz. 1975. A chemical comparison of tropomyosins from muscle and non-muscle tissues. *J. Mol. Biol.* 95:447–454.
54. Schloss, J. A., and R. D. Goldman. 1980. Microfilaments and tropomyosins of cultured mammalian cells: isolation and characterization. *J. Cell Biol.* 87:633–642.
55. Hatano, S. 1970. Specific effect of Ca^{2+} on movement of plasmodial fragment obtained by caffeine treatment. *Exp. Cell Res.* 61:199–203.
56. Kuroda, K. 1979. Movement of cytoplasm in a membrane-free system. *In* Cell Motility: Molecules and Organization. S. Hatano, H. Ishikawa, and H. Sato, editors. University of Tokyo Press, Tokyo. 347–361.
57. Ueda, T., K. Gotz von Olenhusen, and K. E. Wohlfarth-Bottermann. 1978. Reaction of the contractile apparatus in *Physarum* to injected Ca^{++}, ATP, ADP, and 5'AMP. *Cytobiologie.* 18:76–94.
58. Nachmias, V. T., and C. H. Meyers. 1980. Cytoplasmic droplets produced by the effect of adenine on *Physarum* plasmodia. *Exp. Cell Res.* 128:121–126.
59. Kato, T., and Y. Tonomura. 1975. *Physarum* tropomyosin-troponin complex: isolation and properties. *J. Biochem.* (*Tokyo*) 78:583–588.
60. Wang, K., and S. J. Singer. 1977. Interaction of filamin with F-actin in solution. *Proc. Natl. Acad. Sci. U. S. A.* 74:2021–2125.
61. Schloss, J. A., and R. D. Goldman. 1979. Isolation of a high molecular weight actin-binding protein from baby hamster kidney (BHK-21) cells. *Proc. Natl. Acad. Sci. U. S. A.* 76:4484–4488.
62. Maruta, H., and E. D. Korn. 1977. Purification from *Acanthamoeba castellanii* of proteins that induce gelation and syneresis of F-actin. *J. Biol. Chem.* 252:399–402.
63. Davies, P. J. A., D. Wallach, M. C. Willingham, I. Pastan, M. Yamaguchi, and R. Robson. 1978. Filamin-actin interaction: dissociation of binding from gelation by Ca^{2+}-activated proteolysis. *J. Biol. Chem.* 253:4036–4042.
64. Wang, K. 1977. Filamin, a new high-molecular weight protein found in smooth muscle and nonmuscle cells: purification and properties of chicken gizzard filamin. *Biochemistry.* 16:1857–1865.
65. Wallach, D., P. J. A. Davies, and I. Pastan. 1978. Purification of mammalian filamin. *J. Biol. Chem.* 253:3328–3335.
66. Stossel, T. P., and J. H. Hartwig. 1976. Interaction of actin, myosin, and a new actin-binding protein of rabbit pulmonary macrophages II: role in cytoplasmic movement and phagocytosis. *J. Cell Biol.* 68:602–619.
67. Sodeck, J., R. S. Hodges, L. B. Smillie, and L. Jurasek. 1972. Amino-acid sequence of rabbit skeletal tropomyosin and its coiled coil structure. *Proc. Natl. Acad. Sci. U. S. A.* 69:3800–3804.
68. Kretsinger, R. H., and C. D. Barny. 1975. The predicted structure of the calcium-binding component of troponin. *Biochim. Biophys. Acta.* 405:40–52.
69. Matsumura, F., and S. Hatano. 1978. Reversible superprecipitation and bundle formation of plasmodium actomyosin. *Biochim. Biophys. Acta.* 533:511–523.
70. Hinssen, H., and J. D'Haese. 1976. Synthetic fibrils from *Physarum* actomyosin: self assembly, organization and contraction. *Cytobiologie.* 13:132–157.
71. Cummins, P., and S. V. Perry. 1973. The subunits and biological activity of polymorphic forms of tropomyosin. *Biochem. J.* 133:765–777.
72. Hartshone, D. J., and M. Aksoy. 1977. Biochemistry of the contractile proteins in smooth muscle: a survey of current knowledge. *In* The Biochemistry of Smooth Muscle. N. L. Stephens, editor. University Park Press, Baltimore, London, and Tokyo. 363–378.
73. Ogihara, S. 1982. Calcium and ATP regulation of the oscillatory torsional movement in a Triton model of *Physarum* plasmodial strands. *Exp. Cell Res.* In press